Scientific Research

Triterpenes from *Cabralea canjerana* as *in Vitro* Inhibitors to Light Reactions of Photosynthesis

Beatriz King-Díaz[1], Márcio S. Soares[2], Maria Fátima das G. F. da Silva[3], Blas Lotina-Hennsen[1*], Thiago A. M. Veiga[4*]

[1]Departamento de Bioquímica, Facultad de Química, Universidad Nacional Autónoma de México (UNAM), Ciudad Universitaria, México D. F., México
[2]Universidade Federal de Viçosa (UFV), Rio Paranaíba, Brasil
[3]Departamento de Química, Universidade Federal de São Carlos (UFSCar), São Carlos, Brasil
[4]Instituto de Ciências Ambientais, Químicas e Farmacêuticas, Departamento de Ciências Exatas e da Terra, Universidade Federal de São Paulo (UNIFESP), Diadema, Brasil
Email: [*]blas@servidor.unam.mx, [*]tveiga@unifesp.br

Abstract

Aims: Cabraleadiol (1), Ocotilone (2) and Odoratone (3) are three triterpenes isolated from *Cabralea canjerana* (Vell.) Mart. (Meliaceae). They were chemically characterized, and their effect was tested on the light reaction of photosynthesis. Study Design: Natural products were used as models to find new models for inhibitors of photosynthesis. Place and Duration of Study: Departmento de Química, Universidade Federal de São Carlos and Departmento de Bioquímica, Facultad de Química, Universidad Nacional Autonoma de México, between May 2013 and January 2014. Methodology: The natural products had their effect on the light reaction of photosynthesis studied by pollarography and Chlorophyll a (Chl *a*) fluorescence transients. Results: The compounds inhibited ATP synthesis and electron transport rate (basal, phosphorylating and uncoupled). Therefore, they act as Hill reactions inhibitors. Their inhibition site were located in the range of electron flow from OEC complex and between P_{680} to Q_A of PS II, and inhibited the photosystem II (PS II) by inducing the appearance of a K-band which is an indicative that the photochemical apparatus is failing at the donor side of PS II interacting at the OEC complex and by transforming active reaction centers to "heat sinks" or the formation of silent reaction centers unable to reduce Q_A. Conclusion: Furthermore, these triterpenes inhibit PS II and induce the appearance of small G band which is related with the decreased plastoquinone (PQ) pool reduction.

---

[*]Corresponding authors.

How to cite this paper: King-Díaz, B., Soares, M.S., da Silva, M.F.G.F., Lotina-Hennsen, B. and Veiga, T.A.M. (2014) Triterpenes from *Cabralea canjerana* as *in Vitro* Inhibitors to Light Reactions of Photosynthesis. *American Journal of Plant Sciences*, **5**, 2528-2540. http://dx.doi.org/10.4236/ajps.2014.516267

1. Introduction

Photosystem II (PS II) is the membrane-protein complex which catalyses electron transfer from water to plastoquinone. The PS II complex consists of more than 20 proteins and six different active cofactors, including chlorophyll and a manganese site which is required for water oxidation. PS II electron transfer starts with the excitation of the reaction centre chlorophyll *a* species P_{680} to P_{680}^*, and rapid electron transfer away from P_{680}^*, via pheophytin, to the bound plastoquinone, Q_A, to form the pair $P_{680}^+ Q_A^-$. Electron transfer then occurs from Q_A to a second plastoquinone, Q_B. Following two turnovers, Q_B has accepted two electrons and taken up two protons [1]-[3]. $Q_B H_2$ dissociates from its site into the membrane *pool* of plastoquinone and is replaced by a new molecule of Q_B. P_{680}^+ extracts an electron from the oxygen evolution complex (OEC), via the electron donor Y_Z, tyrosine-161 on the D1 polypeptide.

In the acceptor-side of PS II [4]-[6], photoinhibition is assumed to start when the plastoquinone *pool* connecting the two photosystems is reduced under intense light. Experiments leading to the formulation of the acceptor-side were done by illuminating PS II membranes with strong light under anaerobic conditions [5], where the Q_A electron acceptor of PS II stays mainly in the reduced form and the reduced state can be stabilized by protonation or double reduction.

On the other hand, the light-dependent photophosphorylation is coupled to electron transport rate and can be inhibited by different ways: by blocking the electron transport, by direct inhibition of the H^+-ATPase, or by uncoupling the ATP synthesis process from the electron transport [7]. Within this context, several researchers reported the effects of different types of natural products as inhibitors of photosynthesis. Torres-Romero *et al.* in 2008 [8], found three sesquiterpenes that behave as Hill reaction inhibitors and weak energy transfer inhibitors and have two targets of interaction: one located at the oxygen-evolving complex, and the other located at the light-activated Mg^{2+}-ATPase. The ambiguine D isonitrile caused increased reactive oxygen species (ROS) generation and was associated with observed lipid peroxidation and cell death. These oxidative processes probably play a key role in the phytotoxic action [9].

Three pentacyclic triterpenes isolated from *Xylosma flexuosa* had different mechanisms of action on photosynthesis. It acts as energy transfer inhibitors, interacting with isolated CF1 bound to thylakoid membrane, Hill reaction inhibitors and as an uncoupler, as determined by polarographic measurements [10]. Lupane triterpenes isolated from *Melilotus messanensis* possess potential allelopathic activity in particular on dicotyledonous species [11], and the 3,4-secofriedelan-3-oic acid produced by *Maytenus imbricata* has been reported to inhibit several photosynthetic activities [12]. Various friedelane triterpenoids were evaluated for their photosynthetic inhibitory activity. The *in vivo* assays indicated that epifriedelinol and canophyllol act as selective post emergence herbicides at 100 μM by reducing biomass production in the weed *Physalis ixocarpa* [13].

Continuing with our studies [10] [13] [14] to find natural products with biological activity, we isolated a series of triterpenes from *Cabralea canjerana* (**Figure 1**). The chemical profile of Meliaceae family has found several types of compounds, like: coumarins, terpenoids and also many limonoids which were found frequently. Our aim is characterizing natural compounds that affect photosynthesis as a target and mechanism of phytotoxicity *in vitro*. We report here the effect of cabraleadiol (**1**), ocotillone (**2**) and odoratone (**3**) (**Figure 1**), on several photosynthetic activities to help us to elucidate their mechanism of actions in isolated spinach chloroplasts, measured with polarographic techniques and fluorescence induction curves of chlorophyll *a* (Chl *a*) of PS II.

2. Material and Methods

2.1. Tested Material

Three natural triterpenes (**1** - **3**) were isolated from the ethanol extracts of the seeds and fruits of *Cabralea canjerana* (Vell.) Mart. (Meliaceae) as previously has been published [15]-[20]. Stock solutions for compounds **1** - **3** were prepared using a DMSO (dimethyl sulfoxide, the maximum concentration of solvent mixture in the media
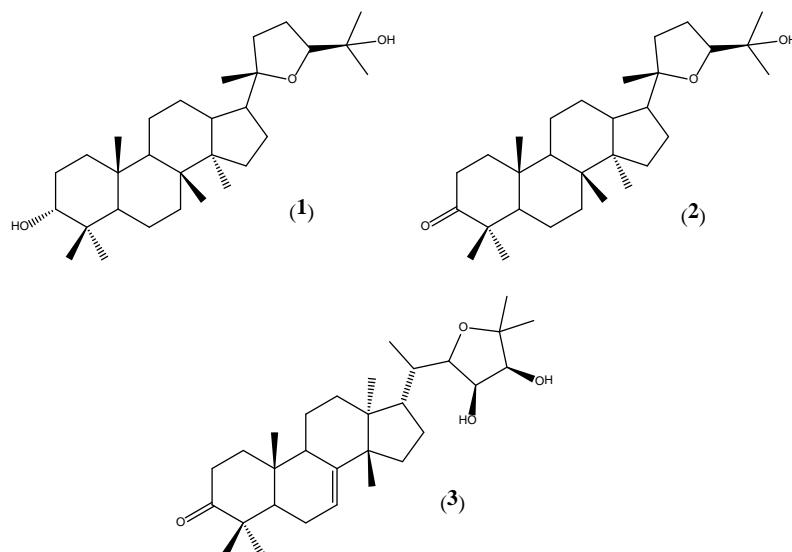
Figure 1. Studied triterpenes isolated from *C. canjerana*.

was less than 1%).

2.2. Isolation of Natural Products

The ethanol extract (70.0 g) of the fruits of *C. canjerana* was subjected to a liquid-liquid extraction with a 120 mL of solution (methanol-water [1:3]). The solution was extracted with different solvents to give us fractions in hexane (47.4 g), dichloromethane (5.4 g), ethyl acetate (4.4 g) and methanol (11.9 g). On the other hand, the ethanolic extract (14.3 g) of the seeds of *C. canjerana* was subjected to chromatographic column using micro-crystalline cellulose-D (5.0 cm × 22.0 cm) as support. The mobile phase was composed by hexane/dichlorome-thane/ethyl acetate/methanol in ascending order of polarity, giving us eleven fractions.

Cabraleadiol (**1**) and Ocotilone (**2**). These natural products were isolated as follow. The dichloromethane frac-tion (5.4 g) of the fruits of *C. canjerana* was subjected to a silica gel column (230 - 400 mesh, 4.0 cm × 16.0 cm), using hexane/dichloromethane/ethyl acetate/ methanol as mobile phase in ascending order of polarity, producing twenty fractions. The fraction seven (345.0 mg) was applied in a column of sephadex LH-20 (3.2 cm × 64.0 cm), with an isocratic mode of elution (methanol/dichloromethane [1:1]), producing four fractions, from the fraction two was obtained the compound **1** (24.6 mg). ^{1}H NMR (δ, 400 MHz, CDCl$_3$): 3.40 (*t*), H-3; 3.64 (*dd*), H-24; 0.98 (*s*), Me-18; 0.87 (*s*), Me-19; 1.15 (*s*), Me-21; 1.19 (*s*), Me-26; 1.11 (*s*), Me-27; 0.94 (*s*), Me-28; 0.84 (*s*), Me-29; 0.89 (*s*), Me-30. ^{13}C NMR (δ, 100 MHz, CDCl$_3$): 33.6 (C-1); 25.3 (C-2); 76.2 (C-3); 37.6 (C-4); 49.5 (C-5); 18.2 (C-6); 35.1 (C-7); 40.6 (C-8); 50.6 (C-9); 37.2 (C-10); 21.6 (C-11); 27.0 (C-12); 42.7 (C-13); 50.1 (C-14); 31.4 (C-15); 25.8 (C-16); 49.8 (C-17); 15.5 (C-18); 16.0 (C-19); 86.5 (C-20); 27.7 (C-21); 34.7 (C-22); 26.3 (C-23); 86.2 (C-24); 70.2 (C-25); 27.8 (C-26); 24.0 (C-27); 28.3 (C-28); 22.1 (C-29) and 16.5 (C-30).

The fraction five (545.0 mg) was subjected to a chromatographic column (3.0 cm × 26.0 cm) using as statio-nary phase silica gel/florisil (1:1). The mobile phase was formed by hexane/dichloromethane/ethyl acetate/me-thanol in different concentrations, giving us five fractions (A-E). The fraction D produced **2** (85.0 mg). ^{1}H NMR (δ, 200 MHz, CDCl$_3$): 3.63 (*m*), H-24; 0.89 (*s*), Me-18; 0.95 (*s*), Me-19; 1.15 (*s*), Me-21; 1.12 (*s*), Me-26; 1.19 (*s*), Me-27; 1.08 (*s*), Me-28; 1.04 (*s*), Me-29; 1.01 (s), Me-30. ^{13}C NMR (δ, 50 MHz, CDCl$_3$): 39.9 (C-1); 34.6 (C-2); 218.0 (C-3); 47.4 (C-4); 55.3 (C-5); 19.7 (C-6); 34.1 (C-7); 40.3 (C-8); 50.0 (C-9); 36.8 (C-10); 22.3 (C-11); 25.0 (C-12); 43.3 (C-13); 50.2 (C-14); 31.4 (C-15); 26.9 (C-16); 49.8 (C-17); 16.0 (C-18); 15.2 (C-19); 86.5 (C-20); 24.3 (C-21); 34.8 (C-22); 27.1 (C-23); 86.4 (C-24); 70.3 (C-25); 26.8 (C-26); 27.1 (C-27); 26.4 (C-28); 21.0 (C-29) and 16.3 (C-30).

Odoratone (**3**). The fraction II (2.50 g) of the ethanol extract of the seeds of *C. canjerana* was subjected to a silica gel/florisil column (1:1, 4.0 cm × 16.0 cm), using hexane/dichloromethane/ethyl acetate/methanol as mo-bile phase in ascending order of polarity, giving us eleven fractions (I - XI). The fraction III (480 mg) was ap-plied in a column of sephadex LH-20 (2.5 × 70.5 cm), using methanol (100%) as solvent of elution to give us

four fractions. The fraction two gives us the compound **3** (41.0 mg). ^{1}H NMR (δ, 400 MHz, CDCl$_3$): 1.92 (*m*), H-17; 7.59 (*d*), H-23; 3.96 (*m*), H-24; 0.86 (*s*), Me-18; 1.04 (*s*), Me-19; 0.85 (*d*), Me-21; 1.17 (*s*), Me-26; 1.15 (*s*), Me-27; 1.00 (*s*), Me-28; 1.11 (*s*), Me-29; 1.06 (s), Me-30. ^{13}C NMR (δ, 100 MHz, CDCl$_3$): 38.5 (C-1); 34.9 (C-2); 217.1 (C-3); 47.9 (C-4); 52.3 (C-5); 24.3 (C-6); 117.8 (C-7); 146.0 (C-8); 49.3 (C-9); 35.0 (C-10); 18.4 (C-11); 34.0 (C-12); 43.5 (C-13); 51.2 (C-14); 33.5 (C-15); 29.6 (C-16); 48.5 (C-17); 21.9 (C-18); 12.8 (C-19); 37.6 (C-20); 12.3 (C-21); 83.7 (C-22); 77.5 (C-23); 72.9 (C-24); 81.0 (C-25); 29.6 (C-26); 21.3 (C-27); 24.6 (C-28); 21.6 (C-29) and 27.8 (C-30).

2.3. Chloroplasts Isolation and Chlorophyll Determination

Intact chloroplasts were isolated from spinach leaves (*Spinacea oleracea* L.) obtained from a local market as previously described [21] [22]. Chloroplasts were suspended in the following medium: 400 mM sucrose, 5 mM MgCl$_2$, 10 mM KCl, and buffered with 0.03 M Na$^+$-tricine at pH 8.0. They were stored as a concentrated suspension in the dark for 1 h at 4˚C. Intact chloroplasts were efficiently lysed to yield free thylakoids prior to each experiment by incubating them in the following electron transport medium: 100 mM sorbitol, 10 mM KCl, 5 mM MgCl$_2$, 0.5 mM KCN, and 30 mM tricine ((N-tris[hydroxymethyl]methylglicine; N-[2-hydroxy-1,1-bis(hydroxymethyl)ethyl]glycine) buffer (pH 8 with the addition of KOH). Chlorophyll concentration was measured spectrophotometrically as reported [23] [24].

2.4. ATP Synthesis

ATP synthesis was determined titrametrically using a microelectrode (Orion model 8103 Ross) connected to a Corning potentiometer model 12, with expanded scale as reported elsewhere [25]. The ATP synthesis reaction medium contained 100 mM sorbitol, 10 mM KCl, 5 mM MgCl$_2$, 0.5 mM KCN, and 1 mM K$^+$-tricine (pH 8.0), 50 μM methylviologen (MV) was used as electron acceptor. Chloroplasts were added to a final concentration of 20 μg chlorophyll/mL. The reaction was started by illumination the chloroplasts with saturating light.

2.5. Measurement of Non-Cyclic Electron Transport Rate

Light-induced non-cyclic electron transport activity from water to MV was determined by using a Clark type electrode, as published, in the presence of 50 μM of MV as electron acceptor [26]. Basal electron transport was determined by illuminating chloroplasts during 1 min (equivalent of 20 μg/mL of chlorophyll) were lysed in 3.0 mL of the reacting medium: 100 mM sorbitol, 5 mM MgCl$_2$, 10 mM KCl, 0.5 mM KCN, 30 mM Na$^+$-tricine, and 50 μM MV at pH 8.0. The sample was illuminated in the presence or absence of 6 mM NH$_4$Cl [27]. Phosphorylating non-cyclic electron transport was measured as basal non-cyclic electron transport except that 1 mM ADP and 3 mM KH$_2$PO$_4$ were added to the reaction medium. Uncoupled electron transport from water to MV was tested in the basal non-cyclic electron transport medium, and 6 mM NH$_4$Cl was added. All reaction mixture was illuminated with actinic light of a projector lamp (GAF 2660) passed through a 5 cm filter of a 1% CuSO$_4$ solution for 1 min.

2.6. Uncoupled Photosystem II (PS II) and Photosystem I (PS I). Electron Flow Determination

Electron transport activity was monitored with an YSI (Yellow Springs Instrument) model 5300 oxygen monitors using a Clark type electrode. The reaction medium was the same as in electron transport assay. Uncoupled PS II from H$_2$O to DCPIP (2,6-dichlorophenol indophenol) was measured by the reduction of DCPIP supported O$_2$ evolutions monitored polarographically. The reaction medium for assaying PS II activity contained the same basal electron transport medium in the presence of 1 μM DBMIB (2,5-dibromo-3-methyl-6-isopropyl-1,4-*p*-benzoquinone), 100 μM DCPIP/300 μM K$_3$[Fe(CN)$_6$], and 6 mM NH$_4$Cl. Uncoupled PSI electron transport from reduced DCPIP with Na$^+$-ascorbate to MV was determined in a similar form to basal non-cyclic electron transport medium. The following reagents were added: 10 μM DCMU (3-(3,4-dichlorophenyl)-11-dimethylurea), 100 μM DCPIP, 50 μM MV, 300 μM ascorbate, and 6 mM NH$_4$Cl. Uncoupled PS I electron transport from reduced PMS (phenylmetasulfate) to MV was determined using KCN poisoned chloroplasts. The reaction medium was the same as in photosystem I except that 500 μM PMS/100 μM ascorbate was used as electron donor to P$_{700}$ (PS I reaction center), MV as PS I electron acceptor, 10 μM DCMU as inhibitor to Q$_B$ (secondary quinone elec-

tron acceptor of PS II), and 6 mM NH_4Cl used as uncoupler to PS I. Cyanide treated chloroplasts were prepared by incubating chloroplasts for 30 min at 4°C in 30 mM KCN and then centrifuged at 8000*g* (Sorvall super T21) for 1 min and resuspended in the reaction medium [26]. Moreover, EPR (electron paramagnetic resonance) spectroscopy confirmed the ability of reduced PMS to interact directly with P_{700}. The I_{50} value for each activity was extrapolated using the graph of percent activity versus concentration of compounds. I_{50} is the concentration to produce 50% of inhibition.

2.7. Chlorophyll *a* Fluorescence Determination

Chlorophyll *a* fluorescence was measured with a Hansatech Fluorescence Handy PEA (plant efficiency analyzer) in 10 min dark-adapted chloroplasts (20 μg/ml) at room temperature at 200 μM of triterpens [21] [28], using red light intensity (broad band 650 nm) of 2800 μmol·m^{-2}·s^{-1}, provided by an array of three light emitting diodes. The pulse duration was 2 s. To monitor Chl *a* fluorescence transients, aliquots of dark adapted thylakoids were placed by gravity on filter paper with a dot-blot apparatus (Bio-Rad, United States) to ensure a homogeneous and reproducible distribution of thylakoids in the filter paper, then the filter paper were dipped immediately in 3 mL of electron transport medium with 200 and 800 μM of the tested compound, the reaction medium used was as the same employed in basal non-cyclic electron transport measurements.

3. Results and Discussion

3.1. ATP Synthesis

To know if the triterpenes **1** - **3** inhibit ATP synthesis, all of them were assayed on photophosphorylation activity coupled to electron transport from water to MV in isolated freshly lysed spinach chloroplasts. **Figure 2** shows that at increasing concentrations of the triterpenes, the synthesis of ATP decreased. The I_{50} values were 35.0, 17.5 and 67.0 μM for **1**, **2** and **3**, respectively.

3.2. Effect of the Triterpenes 1 - 3 on Electron Transport Rate from Water to MV in Chloroplasts

To know the mechanism of inhibition of triterpenes on ATP synthesis coupled to electron transport (basal, phosphorylating, and uncoupled), electron transport rate from water to MV was determined in freshly lysed spinach chloroplasts. We explored whether the effects on ATP synthesis could be inhibited by blockage of the electron transport within the thylakoid chain, by direct inhibition of the H^+-ATPase complex or by dissipation of the H^+-gradient, with are uncoupling effect [7]. **Figures 3-5** show the effects of **1**, **2**, and **3** on chloroplast electron transport rate in its three states (basal, phosphorylating and uncoupled) showing I_{50} values for uncoupled
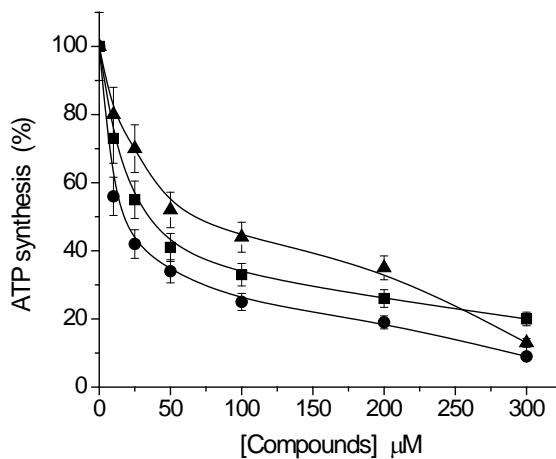

Figure 2. Inhibiting effect of terpenes 1 (■), 2 (●) and 3 (▲) on ATP synthesis. Control value = 100 % = 750 *μM* ATP/mg of Chl × h. Results are the average of three replicates.
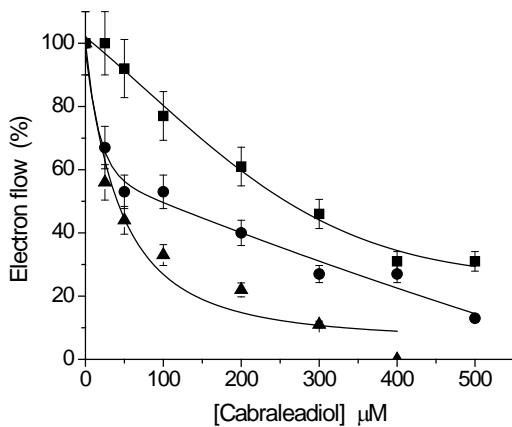
Figure 3. Effect of terpene cabraleadiol (1) on electron transport flow: basal (■); phosphorylating (●); uncoupled (▲). Control = 100% = 400, 650, and 920 μequiv of e^- $\times$ mg^{-1} of $Chl \times h$, respectively. Each curve is the average of three replicates.
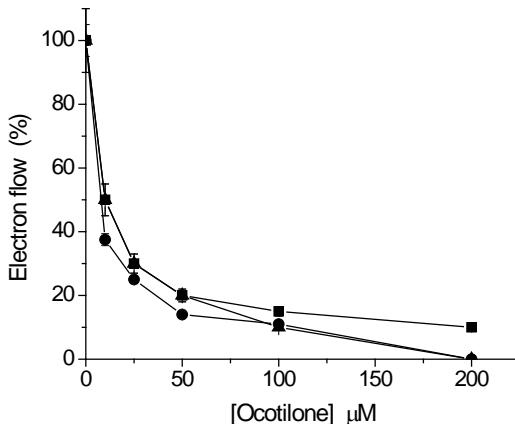

Figure 4. Effect of terpene ocotilone (2) on electron transport flow: basal (■); phosphorylating (●), and uncoupled (▲). Control = 100% = 760, 680, and 880 μequiv of $e^- \times$ mg^{-1} of $Chl \times h$, respectively. Each curve is the average of three replicates.

electron flow of 41, 10 and 47 μM for **1**, **2** and **3,** respectively, being **2** the most active electron transport flow inhibitor. These results indicate that **1** - **3** act as Hill reaction inhibitors. To know one of the physicochemical property of the natural products, the Log P values was calculated with the program ACD/ChemSketch and their values were 7.90 ± 0.42, 7.33 ± 0.46 and 6.95 ± 0.51 for triterpenes **1**, **2** and **3**, respectively, in this case the compound with the major Log P shows minor activity as Hill reaction inhibitor, however compound **2** with the middle Log P value was the most active, may be this Log P value of **2** is the required to reach the target for inhibition.

To localize the action site of **1** - **3** on non-cyclic electron transport chain of chloroplasts, their effects on partial reactions of PS II and PS I were tested using appropriate artificial electron donors, electron acceptors, and electron transport inhibitors [26] [29]. **Table 1** shows that the compound **1** partially inhibited uncoupled PS II electron transport from water to DCPIP (from H_2O to Q_B), from water to SiMo (from H_2O to Q_A) and PS II from DPC to DCPIP (from P680 to Q_B) as concentrations increases, **2** and **3** inhibited 100% at 400 µM electron flow of PS II measured from H_2O to DCPIP and H_2O to SiMo, and partial reaction from DCPIP to DPC was partially inhibited by the triterpenes. These results indicate that the interaction and inhibition site of **1 - 3** are located at the water splitting enzyme complex and between the range of electron flow from P_{680} to Q_A of the PS II electron
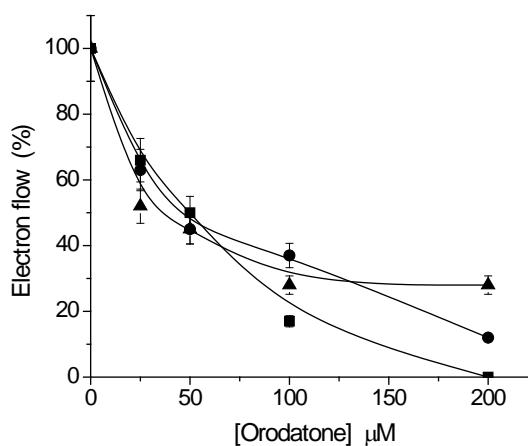
Figure 5. Effect of the terpene orodatone (3) on electron transport flow: basal (■); phosphorylating (●); uncoupled (▲). Control = 100% = 756, 533, and 355 μequiv of e$^-$ × mg^{-1} of Chl × h, respectively. Each curve is the average of three replicates.

Table 1. Effects of triterpenes [1]-[3] on PS II electron flow and its partial reactions.

Comp/ Conc	H$_2$O to DCPIP		H$_2$O to SiMo		DCPIP to DPC	
	μequiv e$^-$·mg^{-1} Chl	%	μequiv e$^-$·mg^{-1} Chl	%	μM DCPIP$_{red}$ mg^{-1} Chl·h^{-1}	%
1/μM	440 ± 22.0	100	215 ± 10.7	100		
0	317 ± 15.8	72	193 ± 9.7	90	0.754 ± 0.04	100
100	268 ± 13.4	61	172 ± 8.6	80	0.702 ± 0.03	93.2
200	238 ± 11.9	54	129 ± 6.4	60	0.608 ± 0.03	80
300	158 ± 7.9	36	86 ± 2.0	40	0.456 ± 0.02	60
2/μM	400 ± 20.0	100	222 ± 11.0	100		
0	184 ± 9.2	46	172 ± 8.9	80	0.702 ± 0.03	100
100	124 ± 6.0	31	151 ± 7.7	70	0.530 ± 0.03	75
200	60 ± 3.0	15	86 ± 4.4	40	0.378 ± 0.02	54
	0	0	0	0	0.332 ± 0.02	47
3/μM	400 ± 20.0	100	222 ± 11.0	100		
0	244 ± 12.3	61	161 ± 8.3	75	0.702 ± 0.03	100
100	216 ± 10.8	54	107 ± 5.5	50	0.576 ± 0.04	82
200	124 ± 6.1	31	82 ± 4.2	38	0.518 ± 0.04	74
	0	0	0	0	0.466 ± 0.04	66

transport chain, because reduced DPC donates electrons to P$_{680}$ [30]. Triterpenes have no effects on PS I electron flow measured from reduced DCPIP to MV (data not shown).

3.3. Chlorophyll *a* Fluorescence Transient Measurements in the Presence of Triterpenes

To corroborate the interaction site of triterpenes at PSII, freshly lysed chloroplasts were incubated for 5 min in the dark at room temperature at 200 μM of the compounds, 10 μM DCMU, and 0.8 M Tris, which were used as positive controls (**Figure 6**). The thylakoids control showed a polyphasic fluorescence curve with OJIP sequence of transients similar to that previously described for plants, green algae, and cyanobacteria [28]; the addition of 10 μM of the herbicide DCMU induces a fast rise of the fluorescence yield during the first 2 ms of illumination; it transforms the regular OJIP sequence into an OJ curve (**Figure 6**) [28]. When the thylakoids are treated with Tris, a well-known donor side of PS II inhibitor [31] (**Figure 6**), the fluorescence induction curve change and the maximum fluorescence yield was reduced and the K-band appears, a rapid rise to a maximum (at 300 μs) followed by a decreased fluorescence yield to level close to F_0 (**Table 2**). All other steps, J and I are absent from the transient [32] [33]. The tris-treated thylakoid conditions are shown also by heat-treated chloroplasts where the OEC damage occurs.

The **Figure 7** shows the effects of the triterpenoids applied at the major concentration (200 μM) on the fluorescence induction curves compared with the control; Compound **2** shows the major effect on the OJIP curve
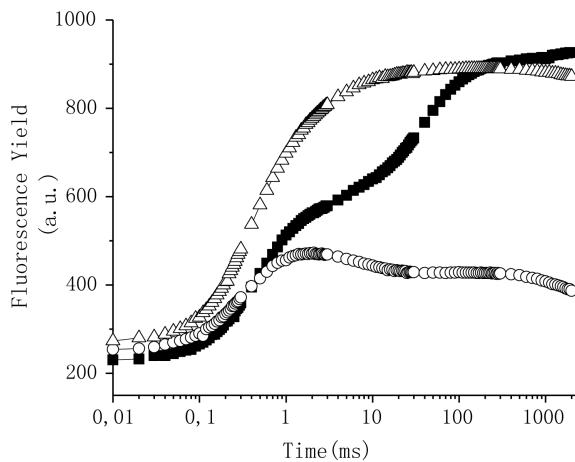
Figure 6. Fluorescence of Chl *a* rise kinetics of freshly lysed broken chloroplasts infiltrated with 10 μM DCMU ($\triangle$), and tris-treated thylakoids (O). Control chloroplasts (■) are shown for comparison. Chl *a* fluorescence induction curves were measured at room temperature. Details are in Materials and Methods. Data are averages of five replicates.
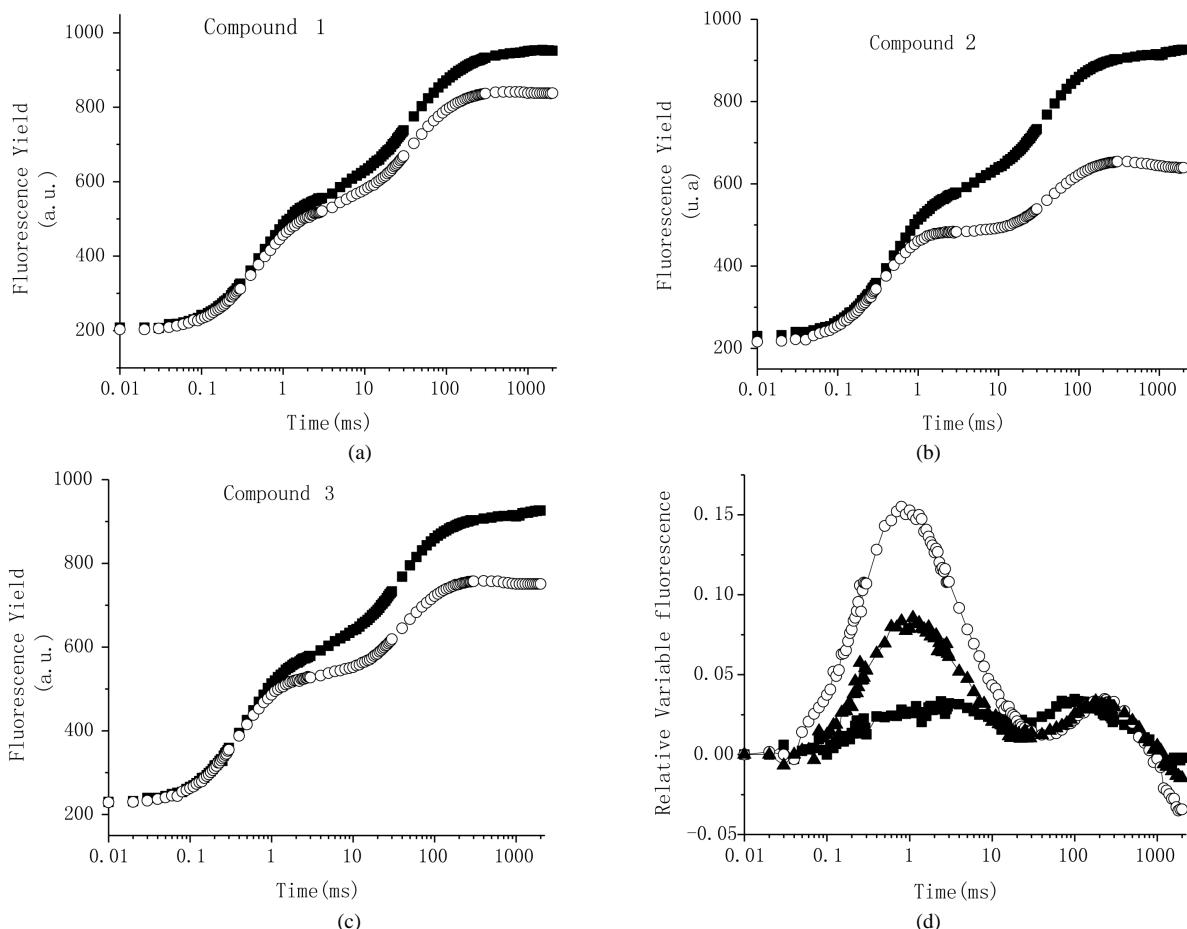

Figure 7. Effect of the compounds at 200 µM, (panel (a)) 1, (panel (b)) 2 and (Panel (c)) 3 on the OJIP curves, close symbols represent control and open symbols are the samples treated with the terpenoids. Panel D shows bands K (0.3 ms) and G (near 300 ms) obtained with the normalized relative variable fluorescence of chlorophyll *a* of thylakoids infiltrated with 200 µM of terpenoids 1 (■), 2 (O) and 3 (▲). Each curve is an average of five replicates.

Table 2. Experimental average values ± standard deviation of chlorophyll *a* fluorescence obtained in control and treated chloroplasts with DCMU, tris buffer and natural products at 200 μM. The values correspond to traces in **Figure 6** and **Figures 7(a)-(c)**.

	F_0	F_M	F_1	F_2	F_3	F_4	F_5
Control	230 ± 23	926 ± 92	244 ± 24	266 ± 26	359 ± 35	563 ± 56	733 ± 74
0.8 M TRIS	254 ± 25	473 ± 47	270 ± 27	290 ± 30	372 ± 37	471 ± 46	429 ± 43
50 μM DCMU	273 ± 27	890 ± 89	295 ± 30	327 ± 32	481 ± 48	777 ± 78	881 ± 89
Control	208 ± 20	954 ± 95	218 ± 21	242 ± 24	326 ± 32	541 ± 52	738 ± 74
(**1**) 200 μM	203 ± 20	841 ± 84	213 ± 21	232 ± 23	312 ± 31	506 ± 50	669 ± 67
Control	230 ± 23	926 ± 92	244 ± 24	266 ± 26	359 ± 35	563 ± 56	733 ± 74
(**2**) 200 μM	216 ± 21	654 ± 65	231 ± 23	255 ± 25	344 ± 34	481 ± 48	539 ± 54
(**3**) 200 μM	229 ± 22	758 ± 75	241 ± 24	263 ± 26	355 ± 35	521 ± 53	619 ± 62

reducing the maximum fluorescence approximately by one third (**Figure 7(b)**). Analysis of the difference of each curve from control on relative variable fluorescence when the OP phase was normalized between $F_M - F_0 = Vt = (F_t - F_0)/(F_M - F_0)$, shows a K-band (**Figure 7(d)**), being bigger for compounds **2** and **3**, and lower for **1**, this band is an indicative that the compounds **2** and **3** damaged the water splitting enzyme system [34]. However, **1** affect this OEC site but in minor proportion. Furthermore, a band in the IP region appeared (near to 300 ms) (**Figure 7(d)**). And, the derived parameters from the transients obtained with the substances (**Table 3**), were decreased by **2** and **3**, *i.e.* the yields as φ_{Po} decreased in 11 and 7%, φ_{Eo} 32.5 and 20%, and ψ_{Eo} decreased 25 and 14 % with both compounds, respectively (**Figure 8**); the most affected parameter was the performance index up to the PS I end electron acceptors (PI_{Total}), this parameter was decreased 60 % by **2** and 27% by **3**, but **1** has no-effect on it. Parameters as φ_{Do}, δRo, ABS/RC, TRoRC and Mo were increased, being the most affected the parameters Mo and φ_{Do}, they were increased 148 and 29% respectively by **2**. The absorption by reaction center (ABS/RC) increased 40 and 20% with **2** and **3** respectively.

Compound **1** also affect these parameters but in minor proportion (**Figure 8**). These results show that the absorption by reaction center is increased due to damage on the donor site of PSII induced by **2** and **3** and in minor extent by **1**. **Table 4**, shows the fraction of active reaction centers after the treatment with the compounds at 200 μM and calculated as $[(ABS/RC)_C/(ABS/RC)_T \times 100]$, where $(ABS/RC)_C$ means for control value and the $(ABS/RC)_T$ means the treatments values. These results corroborate that **1**, **2** and **3** (200 μM) affect the donor side of PSII by transforming active reaction centers to "heat sinks" (silent reaction centers) or non active reaction centers. In the other hand, the small band in the I-P region appeared (near to 300 ms), G band appears (**Figure 7**, Panel D) and it is related with the plastoquinone (PQ) pool reduction, indicating that the terpenoids decreases the available electrons to reduces Q_A, as well as, the PQ pool as a consequence of the formation of non active reaction centers. The compound **2** was most potent as inhibitors than **1**. The difference in structures between **1** and **2** is the presence of the carbonyl group at C3 of **2**, which may be is necessary for activity, while at the compound **1** have a hydroxyl group. On the other hand, odoratol had its mechanism of action site located at the donor side of PS II [14] and the (I_{50}) value on ATP synthesis for odoratol was 67 μM. This compound has a similar structure to odoratone (**3**), which had a calculated I_{50} value of 35 μM. Thus, we can suggest that the presence of the carbonyl group is very important for inhibition and increases the potency of the natural product on photosynthesis and suggest that will be useful for herbicidal activity.

4. Conclusion

In this study we have demonstrated that three triterpenes (**1** - **3**) isolated from *Cabralea canjerana*, act as a Hill reaction inhibitors in a similar way as other natural products such as lasiodiplodin [35] and siderin [36]. Polarographic measurements and chlorophyll a fluorescence measurements indicate that **2** and **3** inhibited partially the water-splitting enzyme, and have their sites of interaction localized the range electron transport from P680 to QA and also inhibited the donor side of PS II, at the OEC complex. Therefore, these compounds may be good candidates as lead structures, which could be optimized for the development of new herbicides.

Table 3. Derived parameters, their description and formulae using data extracted from the chlorophyll *a* fluorescence (OJIP) transient presented in this work.

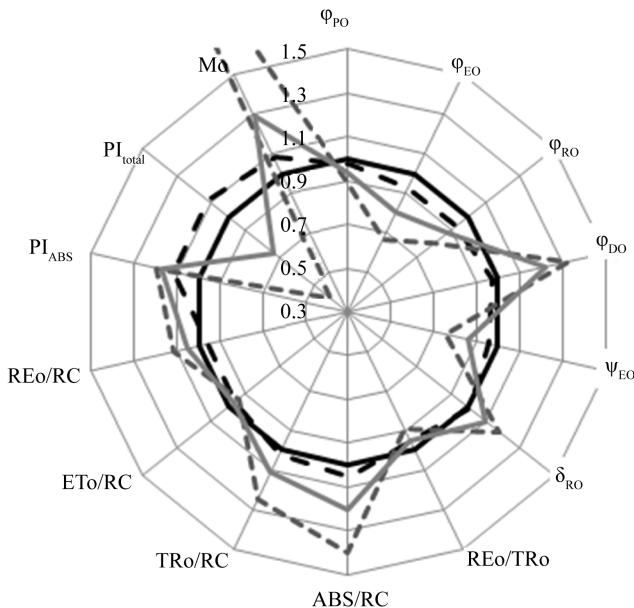| *Fluorescence parameters derived from the extracted data*	
$M_0 = 4(F_{300\mu s} - F_0)/(F_M - F_0)$	Approximated initial slope (in $m \cdot s^{-1}$) of the fluorescence transient $V = f(t)$
Yields or flux ratios	
$\varphi_{Po} = TR_0/ABS = [1 - F_0/F_M]$	Maximum quantum yield of primary photochemistry at $t = 0$
$\varphi_{Eo} = ET_0/ABS = [1 - (F_J/F_M)]$	Quantum yield for electron transport at $t = 0$
$\varphi_{Ro} = RE_0/ABS = \varphi_{Po}\psi_{Eo}\delta_{Ro} = 1 - (F_I/F_M)$	Quantum yield for the reduction of end acceptors of PSI per photon absorbed
$\varphi_{Do} = 1 - \varphi_{Po} = F_0/F_M$	Quantum yield (at $t = 0$) of energy dissipation
$\psi_{Eo} = ET_0/TR_0 = (1 - V_J)$	Probability (at $t = 0$) that a trapped exciton moves an electron into the electron transport chain beyond Q_A^-
$\delta_{Ro} = RE_0/ET_0 = (1 - V_I)/(1 - V_J)$	Efficiency with which an electron can move from the reduced intersystem electron acceptors to the PS I end electron acceptors of PS I
$RE_0/TR_0 = \psi_{Eo}\delta_{Ro}$	Efficiency with which a trapped exciton move an electron into the electron transport chain from Q_A^- to the PS I end electron acceptors
Specific fluxes or activities per reaction center (RC)	
$ABS/RC = M_0(1/V_J)(1/\varphi_{Po})$	Absorption per RC
$TR_0/RC = M_0/V_J$	Trapped energy flux per RC (at $t = 0$)
$ET_0/RC = M_0(1/V_J)\psi_{Eo}$	Electron transport flux per RC (at $t = 0$)
$RE_0/RC = (RE_0/ET_0)(ET_0/RC)$	Reduction of end acceptors at PSI electron acceptor side per RC at $t = 0$
Performance index	
$PI_{ABS} = \dfrac{RC}{ABS} \times \dfrac{TR_0}{ABS - TR_0} \times \dfrac{ET_0}{TR_0 - ET_0}$	Performance index on absorption basis
$PI_{total} = PI_{ABS} \times \dfrac{\varphi_{R_0}}{1 - \delta_{R_0}} = \dfrac{RE_0}{ET_0 - RE_0}$	Total PI, measuring the performance up to the PS I end electron acceptors

Figure 8. Radar plot showing the effect of 200 µM of terpene 1 (black dashed line), 2 (grey dashed line), 3 (grey continuous line) of the derived parameters calculated from the OJIP transients presented by dark-adapted freshly lysed chloroplasts. Control is represented by a continuous line at the center of the radar.

Table 4. Active Reaction Centers calculated as [(ABS/RC)C/ABS/(RC)T] $\times$ 100 in control and treated chloroplasts with terpenoids **1** - **3**.

Compound/200 μM	ABS/RC	Active RC (%)
Control	1.8124	100
1	1.8970	95.54
Control	2.06	100
2	2.88	71.5
Control	2.06	100
3	2.4730	83.0

Acknowledgements

Competing Interests

Authors have declared that no competing interests exist.

References

[1] Diner, B.A. and Babcock, G.T. (1996) Oxygenic Photosynthesis: The Light Reactions. Kluwer Academic Publishers, Dordrecht, 213-247.

[2] Britt, R.D. (1996) Oxygenic Photosynthesis: The Light Reactions. Kluwer Academic Publishers, Dordrecht, 137-159.

[3] Nugent, J.H.A., Rich, A.M. and Evans, M.C.W. (2001) Photosynthetic Water Oxidation: Towards a Mechanism. *Biochimica et Biophysica Acta* (*BBA*)-*Bioenergetics*, **1503**, 138-146. http://dx.doi.org/10.1016/S0005-2728(00)00223-1

[4] Tyystjarvi, E. (2008) Photoinhibition of Photosystem II and Photodamage of the Oxygen Evolving Manganese Cluster. Coordination Chemistry Reviews, **252**, 361-376. http://dx.doi.org/10.1016/j.ccr.2007.08.021

[5] Vass, I., Styring, S., Hundal, T., Koivuniemi, A., Aro, E.M. and Andersson, B. (1992) Reversible and Irreversable Intermediates during Photoinhibition of Photosystem II: Stable Reduced QA Species Promote Chlorophyll Triplet Formation. *Proceedings of the National Academy of Sciences*, **89**, 1408-1412. http://dx.doi.org/10.1073/pnas.89.4.1408

[6] Vass, I. and Styring, S. (1993) Characterization of Chlorophyll Triplet Promoting States in Photosystem II Sequentially Induced during Photoinhibition. *Biochemistry*, **32**, 3334-3341. http://dx.doi.org/10.1021/bi00064a016

[7] Good, N.E., Izawa, S. and Hind, G. (1981) Current Topics in Bioenergetics. Academic Press, New York, 75-112.

[8] Torres-Romero, D., King-Diaz, B., Jimenez, I.A., Lotina-Hennsen, B. And Bazzocchi, I.L. (2008) Sesquiterpenes from Celastrus Vulcanicola as Photosynthetic Inhibitors. *Journal of Natural Products*, **71**, 1331-1335. http://dx.doi.org/10.1021/np070647y

[9] Koodkaew, I., Sunohara, Y., Matsuyama, S. and Matsumoto, H. (2012) Isolation of Ambiguine D Isonitrile from Hapalosiphon sp. and characterization of Its Phytotoxic Activity. *Plant Growth Regulation*, **68**, 141-150. http://dx.doi.org/10.1007/s10725-012-9700-8

[10] Menezes-de-Oliveira, D., Aguilar, M.I., King-Díaz, B., Vieira-Filho, A.S., Pains-Duarte, L., Silva, G.D.F. and Lotina-Hennsen, B. (2011) The Triterpenes 3β-Lup-20(29)-en-3-ol and 3β-Lup-20(29)-en-3-yl Acetate and the Carbohydrate 1,2,3,4,5,6-Hexa-O-acetyl-Dulcitol as Photosynthesis Light Reactions Inhibitors. *Molecules*, **16**, 9939-9956. http://dx.doi.org/10.3390/molecules16129939

[11] Macıas, F.A., Simonet, A.M. and Esteban, M.D. (1994) Potential Allelopathic Lupane Triterpenes from Bioactive Fractions of Melilotus Messanensis. *Phytochemistry*, **36**, 1369-1379. http://dx.doi.org/10.1016/S0031-9422(00)89726-5

[12] Silva, S.R.S., Silva, G.D.F., Barbosa, L.C.A., Duarte, L.P., King-Dıaz, B., Archundia-Camacho, F. and Lotina-Hennsen, B. (2007) Uncoupling and Inhibition Properties of 3,4-Seco-Friedelan-3-Oic Acid Isolated from Maytenus Imbricata. *Pesticide Biochemistry and Physiology*, **87**, 109-114. http://dx.doi.org/10.1016/j.pestbp.2006.06.008

[13] Torres-Romero, D., King-Diaz, B., Strasser, R.J., Jimenez, I.A., Lotina-Hennsen, B. and Bazzocchi, I.L. (2010) Friedelane Triterpenes from *Celastrus vulcanicola* as Photosynthetic Inhibitors. *Journal of Agricultural and Food Chemistry*, **58**, 10847-10854. http://dx.doi.org/10.1021/jf1022115

[14] Achnine, L., Mata, R., Iglesias-Prieto, R. and Lotina-Hennsen, B. (1998) Impairment of Photosystem II Donor Side by the Natural Product Odoratol. *Journal of Agricultural and Food Chemistry*, **46**, 5313-5317.

http://dx.doi.org/10.1021/jf980589+

[15] Cascon, S.C. and Brown Jr., K.S. (1972) Biogenetically Significant Triterpenes in a Species of Meliaceae: Cabralea Polytricha A. Juss. *Tetrahedron*, **28**, 315-323. http://dx.doi.org/10.1016/0040-4020(72)80138-8

[16] Braga, P.A.C., Soares, M.S., Da Silva, M.F.G.F., Vieira, P.C., Fernandes, J.B. and Pinheiro, A.L. (2006) Dammarane Triterpenes from *Cabralea canjerana* (Vell.) Mart. (Meliaceae): Their Chemosystematic Significance. *Biochemical Systematics and Ecology*, **34**, 282-290. http://dx.doi.org/10.1016/j.bse.2005.10.012

[17] Aalbersberg, W. and Singh, Y. (1991) Tirucallane Triterpenoids from *Dysoxylum hainanense*. *Phytochemistry*, **30**, 921-926. http://dx.doi.org/10.1016/0031-9422(91)85280-D

[18] Tanaka, O. and Yahara, S. (1978) Dammarane Saponins of Leaves of *Panax pseudo-ginseng* subsp. Himalaicus. *Phytochemistry*, **17**, 1353-1358. http://dx.doi.org/10.1016/S0031-9422(00)94588-6

[19] Hisham, A., Bai, M.D.A., Fujimoto, Y., Hara, N. and Shimada, H. (1996) Complete ^{1}H and ^{13}C NMR Spectral Assignment of Cabraleadiol, a Dammarane Triterpene from Dysoxylum Malabaricum Bedd. *Magnetic Resonance in Chemistry*, **34**, 146-150. http://dx.doi.org/10.1002/(SICI)1097-458X(199602)34:2<146::AID-OMR850>3.0.CO;2-U

[20] Mohamad, K., Sevenet, T., Dumontet, V., Pais, M., Tri, V.M., Hadi, H., Awang, K. and Martin, M. (1999) Dammarane Triterpenes and Pregnane Steroids from *Aglaia lawii* and *A. tomentosa*. *Phytochemistry*, **51**, 1031-1037. http://dx.doi.org/10.1016/S0031-9422(99)00053-9

[21] Roux, D., Martin, M.T., Adeline, M.T., Sevenet, T., Hadi, H. and Pais, M. (1998) Foveolins A and B, Dammarane Triterpenes from *Aglaia foveolata*. *Phytochemistry*, **49**, 1745-1748. http://dx.doi.org/10.1016/S0031-9422(98)00305-7

[22] Veiga, T.A.M., King-Díaz, B., Marques, A.S.F., Sampaio, O.M., Vieira, P.C., da Silva, M.F.G.F. and Lotina-Hennsen, B. (2013) Furoquinoline Alkaloids Isolated from *Balfourodendron riedelianum* as Photosynthetic Inhibitors in Spinach Chloroplasts. *Journal of Photochemistry and Photobiology B*: *Biology*, **120**, 36-43. http://dx.doi.org/10.1016/j.jphotobiol.2013.01.006

[23] Morales-Flores, F., Aguilar, M.I., King-Díaz, B. and Lotina-Hennsen, B. (2013) Derivatives of Diterpen Labdane-8α,15-diol as Photosynthetic Inhibitors in Spinach Chloroplasts and Growth Plant Inhibitors. *Journal of Photochemistry and Photobiology B*: *Biology*, **125**, 42-50. http://dx.doi.org/10.1016/j.jphotobiol.2013.04.010

[24] Mills, J.D., Mitchell, P. and Schurmann, P. (1980) Modulation of Coupling Factor ATPase Activity in Intact Chloroplasts. *FEBS Letters*, **191**, 144-148.

[25] Strain, H.H., Cope, T. and Svec, M.A. (1971) Analytical Procedures for the Isolation, Identification, Estimation and Investigation of the Chlorophylls. *Methods in Enzymology*, **23**, 452-476. http://dx.doi.org/10.1016/S0076-6879(71)23118-9

[26] Allen, J.F. and Holmes, N.G. (1986) Photosynthesis: Energy Transduction: A Practical Approach. IRL Press, Oxford, 103-141.

[27] Dilley, R.A. (1972) Ion Transport (H^+, K^+, Mg^{2+} Exchange Phenomena). *Methods in Enzymology*, **24**, 68-74. http://dx.doi.org/10.1016/0076-6879(72)24055-1

[28] Strasser, R.J., Srivastava, A. and Govindjee (1995) Polyphasic Chlorophyll a Fluorescence Transient in Plants and Cyanobacteria. *Photochemistry and Photobiology*, **66**, 32-42. http://dx.doi.org/10.1111/j.1751-1097.1995.tb09240.x

[29] Saha, S., Ouitrakul, R. and Izawa, S. (1971) Electron Transport and Photophosphorylation in Chloroplasts as a Function of the Electron Acceptor. *Journal of Biological Chemistry*, **246**, 3204-3209.

[30] Vernon, L.P. (1969) Photoreduction of 2,6-Dichlorophenolindophenol by Diphenylcarbazide: A Photosystem 2 Reaction Catalyzed by Tris-Washed Chloroplasts and Subchloroplast Fragments. *Plant Physiology*, **44**, 1645-1649. http://dx.doi.org/10.1104/pp.44.11.1645

[31] Rickert, K.W., Sears, J., Beck, W.F. and Brudvig, G.W. (1991) Mechanism of Irreversible Inhibition of O_2 Evolution in Thotosystem II by Tris(hydroxymethyl) Aminomethane. *Biochemistry*, **30**, 7888-7896. http://dx.doi.org/10.1021/bi00246a003

[32] Strasser, R.J. (1997) Donor Site Capacity of Photosystem II Probed by Chlorophyll a Transients. *Photosynthesis Research*, **52**, 147-155. http://dx.doi.org/10.1023/A:1005896029778

[33] Lazár, D., Pospíšil, P. and Naus, J. (1999) Decrease of Fluorescence Intensity after the K Step in Chlorophyll a Fluorescence Induction Is Suppressed by Electron Acceptors and Donors to Photosystem 2. *Photosynthetica*, **37**, 255-265. http://dx.doi.org/10.1023/A:1007112222952

[34] Strasser, R.J., Tsimilli-Michael, M. and Srivastava, A. (2004) Chlorophyll Fluorescence: A Signature of Photosynthesis. Kluwer Academic Publishers, Dordrecht, Chapter 12, 321.

[35] Veiga, T.A.M., Silva, S.C., Archundia-Camacho, F., Rodrigues Filho, E., Vieira, P.C., Fernandes, J.B., da Silva, M.F.G.F., Muller, M.W. and Lotina-Hennsen, B. (2007) Inhibition of Photophosphorylation and Electron Transport Chain in Thylakoids by Lasiodiplodin, a Natural Product from *Botryosphaeria rhodina*. *Journal of Agricultural and*

Food Chemistry, **55**, 4217-4221. http://dx.doi.org/10.1021/jf070082b

[36] Veiga, T.A.M., González-Vásquez, R., Oiano Neto, J., da Silva, M.F.G.F., King-Díaz, B. and Lotina-Hennsen, B. (2007) Siderin from *Toona ciliata* (Meliaceae) as Photosystem II Inhibitor on Spinach Thylakoids. *Archives of Biochemistry and Biophysics*, **465**, 38-43. http://dx.doi.org/10.1016/j.abb.2007.05.002

Scientific Research Publishing (SCIRP) is one of the largest Open Access journal publishers. It is currently publishing more than 200 open access, online, peer-reviewed journals covering a wide range of academic disciplines. SCIRP serves the worldwide academic communities and contributes to the progress and application of science with its publication.

Other selected journals from SCIRP are listed as below. Submit your manuscript to us via either submit@scirp.org or Online Submission Portal.